

Published in final edited form as:

Reprod Toxicol. 2013 July ; 38: 89–101. doi:10.1016/j.reprotox.2013.03.009.

Global gene expression analysis reveals pathway differences between teratogenic and non-teratogenic exposure concentrations of bisphenol A and 17 β -estradiol in embryonic zebrafish

Katerine S. Saili^a, Susan C. Tilton^b, Katrina M. Waters^b, and Robert L. Tanguay^a

^aDepartment of Environmental and Molecular Toxicology, Environmental Health Sciences Center, Oregon State University, Corvallis, OR, 97331, USA

^bComputational Biology and Bioinformatics Group, Pacific Northwest National Laboratory, Richland, WA, 99352, USA

Abstract

Transient developmental exposure to 0.1 μ M bisphenol A (BPA) results in larval zebrafish hyperactivity and learning impairments in the adult, while exposure to 80 μ M BPA results in teratogenic responses, including craniofacial abnormalities and edema. The mode of action underlying these effects is unclear. We used global gene expression analysis to identify candidate genes and signaling pathways that mediate BPA's developmental toxicity in zebrafish. Exposure concentrations were selected and anchored to the positive control, 17 β -estradiol (E2), based on previously determined behavioral or teratogenic phenotypes. Functional analysis of differentially expressed genes revealed distinct expression profiles at 24 hours post fertilization for 0.1 versus 80 μ M BPA and 0.1 versus 15 μ M E2 exposure, identification of prothrombin activation as a top canonical pathway impacted by both 0.1 μ M BPA and 0.1 μ M E2 exposure, and suppressed expression of several genes involved in nervous system development and function following 0.1 μ M BPA exposure.

Keywords

bisphenol A; 17 β -estradiol; microarray; zebrafish; prothrombin; CREB

1. Introduction

Bisphenol A (BPA¹) is a subunit of polymers used in the manufacture of numerous consumer products. Incomplete polymerization or gradual breakdown of BPA-derived materials results in leaching into food or water stored in polycarbonate plastic or resin-lined cans. Chronic, widespread exposure to BPA or its derivatives is thought to occur primarily

© 2013 Elsevier Inc. All rights reserved.

Corresponding author: Robert L. Tanguay, Oregon State University, Department of Environmental and Molecular Toxicology, 28645 East Hwy 34, Corvallis, OR 97333, USA. Telephone: 541-737-6514. Fax: 541-737-6074. Robert.Tanguay@oregonstate.edu.

Publisher's Disclaimer: This is a PDF file of an unedited manuscript that has been accepted for publication. As a service to our customers we are providing this early version of the manuscript. The manuscript will undergo copyediting, typesetting, and review of the resulting proof before it is published in its final citable form. Please note that during the production process errors may be discovered which could affect the content, and all legal disclaimers that apply to the journal pertain.

¹Abbreviations: BPA (bisphenol A), E2 (17 β -estradiol), ER (estrogen receptor), GPER (G-protein coupled estrogen receptor), ERR γ (estrogen-related receptor gamma), hpf (hours post fertilization), dpf (days post fertilization), CRE (cAMP response element)

through ingestion, resulting in average circulating BPA levels ranging from below detectable limits (i.e., < 0.3 [1]) to 3 ng/ml [2]. The 2003/06 NHANES study suggests that detectable BPA exposures may increase risk of heart disease in adults [3], and a recent study correlated BPA exposure with obesity in children [4]. While the true human health risks remain to be determined, studies conducted using experimental models have also implicated BPA exposure in diabetes, reproductive system effects, cancer, and learning impairment [5]. Additional evidence from experimental models indicates that the primary risk posed by BPA exposure might be on organ system development, particularly the central nervous system and prostate, in fetuses or young children [6]. Consistent with these reports, two recent epidemiology studies linked increased levels of BPA during gestation with altered socioemotional behavior in 3–5 year old children [7, 8]. The mode of action underlying developmental BPA toxicity observed in animal models is unclear. As an estrogen disrupting compound, BPA is traditionally thought to act through estrogen receptor (ER) activation. However, it is uncertain whether ER activation alone is sufficient to explain the effects of BPA exposure on organ system development and function. Although BPA is a weak nuclear ER agonist, it is also an agonist of the non-genomic G-protein coupled estrogen receptor (GPER) [9], estrogen-related receptor gamma (ERR γ) [10], and other structurally similar nuclear receptors. The objective of this study was to employ global gene expression analysis to identify BPA-responsive genes downstream of putative BPA receptors as a step toward tracing the route by which BPA exerts its developmental toxicity.

Surprisingly few groups have used microarrays for *in vivo* studies of the effects of BPA exposure on development. Two mouse studies identified sex differences in placental nuclear receptor expression [11] and distinct gene expression profiles in mammary gland following 25 μ g/kg versus 250 μ g/kg oral dose to pregnant dams [12], respectively; while two rat studies identified both shared and distinct gene expression changes in developing reproductive organs following BPA versus 17 α -ethynyl estradiol exposure [13] and distinct differences in 2-week-old uterine gene expression following neonatal BPA versus 17 β -estradiol (E2) exposure, respectively. Only two studies have used non-mammalian models, xenopus and zebrafish, to investigate BPA effects on whole-body mRNA expression during development or early life stages, respectively [14, 15]. The main finding of the xenopus study was that BPA acted as an antagonist of thyroid hormone-responsive genes, while the main finding of the zebrafish study was the identification of genes similarly impacted by BPA and E2 exposure.

We previously observed that developmental BPA exposure results in teratogenic responses at concentrations >30 μ M, specifically yolk sac edema, pericardial edema, and craniofacial abnormalities [16]. We also found that exposure to 0.1 μ M BPA results in significant hyperactivity in 5-day-old larvae and learning impairment in adults exposed as embryos. In comparison, 0.1 μ M E2 exposure also results in significant hyperactivity in 5-day-old larvae and developmental E2 exposure results in morphological defects at concentrations >1 μ M, specifically yolk sac edema, pericardial edema, craniofacial abnormalities, and a “curved tail down” phenotype, with the latter two defects occurring in embryos exposed to >15 μ M [16]. We hypothesized that the overt toxic effects following high concentration exposure and the behavioral impairments associated with lower concentration exposure are engendered through activation of distinct subsets of genes. We also hypothesized that, although the larval hyperactivity phenotype is a common response that can be a manifestation of multiple specific modes of action, at least some shared gene expression changes and signaling pathways underlie BPA- versus E2-induced hyperactivity. To identify which genes and associated signaling pathways putatively underlie these phenotypes, we used a 135K zebrafish microarray analysis to investigate the global gene expression changes associated with 0.1 or 80 μ M BPA and 0.1 or 15 μ M E2 exposure in 24 hours post fertilization (hpf) embryos. These concentrations were selected in part because the associated phenotypes

serve as anchors that allow comparison of gene expression changes despite unidentified differences in BPA and E2 absorption and target receptor binding affinities. The 0.1 μM exposure for both BPA and E2 represents the lowest concentration leading to a measurable phenotype, larval hyperactivity, in a significant number of exposed individuals compared to controls [16]. The higher exposure concentrations, 80 μM BPA and 15 μM E2, were selected specifically because they produce the same morphological defect, yolk sac edema, in a majority of exposed embryos [16]. The selection of the 24 hpf sampling time point was because this is the earliest stage at which the rudiments of all organ systems have developed [17]. Thus, a snapshot of gene expression changes at this time may capture early events initiating a cascade of signaling miscues in multiple organ systems that in turn lead to the common phenotypes. Because this is only a snapshot during a dynamic period of rapid embryonic development, this single sampling time point is intended to serve as a launching platform for future studies including additional time points aimed at more fully characterizing the effects of BPA versus E2 exposure on the multifarious gene expression changes that take place during embryonic development.

2. Materials and methods

2.1. Ethics statement

Zebrafish husbandry and embryo exposures were conducted in compliance with protocols approved by the Oregon State University Institutional Animal Care and Use Committee.

2.2. Chemical exposures

Tropical 5D strain zebrafish were raised at the Sinnhuber Aquatic Research Laboratory at Oregon State University on a recirculating water system at 28 °C on a 14 h/10 h light/dark cycle. One hour post fertilization embryos were obtained from group spawns and incubated in buffered embryo medium at 28 °C until 8 hpf, at which point a homogenous set of viable, age-matched embryos (chorions intact) were loaded individually into the wells of polystyrene 96-well microtiter plates (Becton Dickinson, NJ, USA) using burnished glass pipettes. Chemical stocks were prepared by dissolving bisphenol A (2,2-Bis(4-hydroxyphenyl)propane; 99% purity, Tokyo Chemical Industry America (TCI), Portland, OR) and 17 β -estradiol (Sigma) in dimethylsulfoxide (DMSO; Sigma). One hundred microliters of exposure solution prepared in buffered embryo medium at a final vehicle concentration of 0.1% DMSO were added to each well of the microtiter plates. Plates were sealed with parafilm, covered in foil, and incubated at 28 °C in the dark until 24 or 120 hpf. Subsets of exposed embryos were imaged on a glass slide using an Axiovert 200 M (Zeiss) to depict their morphology at 24 and 120 hpf.

2.3. Microarray sample processing

Glass pipettes were used to collect forty, 24 hpf embryos for each of 3 biological replicates per treatment (N = 2 for 80 μM experiment due to removal of one sample that did not pass quality control). Embryos were pooled in 1.5 ml polypropylene Safe-lock microcentrifuge tubes (Eppendorf, Hamburg, Germany), excess liquid was removed, the pooled embryos were rinsed 3 times with buffered embryo medium, excess liquid was removed, then they were homogenized in 500 μl RNeasy (Molecular Research Center, Inc., Cincinnati, OH, USA; 0.1 μM experiment) or 300 μl TRI ReagentR (Molecular Research Center, Inc., Cincinnati, OH, USA; 80 μM experiment; 200 μl added post-homogenization) using 0.5 mm zirconium oxide beads (~160 mg) and a bullet blender (Next Advance Inc., Averill Park, NY, USA) at speed 8 for 3 minutes. After 5 minutes incubation at room temperature, samples were frozen at -80 °C. Several days later, samples were thawed on ice and RNA was extracted using manufacturer-recommended protocols (the optional DNase treatment step was not included). After precipitation and centrifugation, the total RNA pellet was

washed 3 times in 75% ethanol (EtOH, Koptec, King of Prussia, PA), air dried, and resuspended in RNase/Nuclease free water (Life Technologies, Corp., Grand Island, NY, USA). Total RNA concentration was determined using a Nanodrop spectrophotometer (Thermo Scientific, Waltham, MA, USA) and RNA quality was determined using an Agilent Bioanalyzer 2100 (Agilent Technologies, Inc., Santa Clara, CA, USA). The bioanalyzer quality control step also confirmed the absence of contaminating DNA. An aliquot (13 µg) of each sample was next placed in new tubes, which were sealed in parafilm, enclosed in double ziplock bags, and shipped on dry ice to the NimbleGen Service Processing Facility (Roche NimbleGen, Reykjavik, Iceland).

Sample labeling, microarray hybridization (135K 12-plex zebrafish microarray, Zv7 build; Roche NimbleGen, Inc.), and scanning were all conducted by the processing facility. Probes on the array were 60-mer oligonucleotides with 3 probes per target and 38,489 genes represented per array (www.Nimblegen.com). The lower concentration (0.1 µM BPA and E2) and higher concentration (80 µM BPA and 15 µM E2) samples and respective controls were hybridized to two separate 12-plex microarrays.

2.4. Microarray data analysis

NimbleScan software v2.5 (NimbleGen) was used for image analysis and quality control on samples. Raw intensity data were quantile normalized by RMA summarization [18]. The data discussed in this publication have been deposited in NCBI's Gene Expression Omnibus (GEO) and are accessible through GEO Series Accession number GSE38960 (<http://www.ncbi.nlm.nih.gov/geo/query/acc.cgi?acc=GSE38960>) [19]. Lists of significant differentially expressed genes were generated from the normalized data using GeneSpring GX software (Agilent Technologies, Inc., Santa Clara, CA, USA). Statistical parameters were one-way ANOVA with Tukey's post-hoc test ($p < 0.05$), no False Discovery Rate (FDR) applied, and no fold-change cutoff. Bidirectional hierarchical clustering maps were generated by Euclidean distance in Multi-Experiment Viewer [20]. Annotation of genes was achieved by combining the Zv8 zebrafish genome build and human ortholog IDs from the Vertebrate Genome Annotation Database (VEGA; Wellcome Trust Sanger Institute) using the Bioinformatics Resource Manager [21]. Networks of significant differentially expressed genes were identified using the most current version of Ingenuity Pathway Analysis (IPA; Ingenuity Systems, Inc.) as of August, 2012. Parameters used in IPA were as follows: core analysis, reference set user-defined (i.e., only the set of genes appearing on the microarray and mapped to human Entrez gene ID were included as background reference genes), only direct relationships included, endogenous chemicals included, confidence=experimentally observed or HIGH (predicted), no log ratio cutoff was used, and p-value cutoff was < 0.05 . An upstream regulator analysis, which calculates a regulation z-score and an overlap p-value (Fisher's Exact test; $p < 0.01$) for the comparison of the significant differentially expressed genes in the dataset versus those known to be regulated by a given upstream regulator, was included in the IPA core analysis. The lists of significant canonical pathways and biological functions identified by IPA analysis are included as Tables 1, 2, S1, S2, S4, and S5. Only biological functions with a p-value < 0.01 are shown (Tables S1, S2, S4, and S5). Genes comprising the significant biological function, nervous system development (23), or canonical pathway, prothrombin activation (7), were used to construct the networks shown in Figures 3 and 4. Additionally, 7 genes and 1 micro RNA were manually added from other top networks based on relevance to our hypothesis (*Htr5a*, *Grid1*, *Crebbp*, *Creb*, *Smad3*, *Esr1*, *Hoxa3a*, and miR-132-3p). The basis for including each gene shown in the network is included in Table 3.

The publicly available Database for Annotation, Visualization and Integrated Discovery (DAVID) v6.7 was used to annotate the groups of genes with significant lowered versus elevated expression following exposure for heat map labeling (Figures 2 and 3) [22]. The

DAVID functional annotation tool utilizes the Fisher Exact test to measure gene enrichment in biological process Gene Ontology (GO) category terms for significant genes compared to background, which included all genes on the NimbleGen platform that mapped to human or zebrafish Entrez gene ID. Parameters used in DAVID were as follows: functional annotation clustering analysis; in addition to using default settings, GO terms BP_3, 4, and 5 were added; classification stringency=high. Each GO term label on each heat map represents a single Annotation Cluster, which comprised multiple terms. The reported terms were arranged by enrichment score (highest listed first). Only GO terms with $p < 0.05$ were listed, and redundant terms (either within a category or between two categories) were omitted.

2.5. cAMP response element (CRE) prediction

The CREB Target Gene Database (<http://natural.salk.edu/CREB/>) was searched to determine whether putative CREB-regulated genes have CREs on their promoters. The CRE prediction is based on *in silico* methods that identified CRE binding sites on human genes or animal orthologs. The database also includes data from a ChIP study using human kidney cell line, HEK293T [23].

2.6. Confirmation of microarray gene expression changes

qRT-PCR was used to confirm the expression changes of 3 genes following exposure to either 0.1 μM BPA (*Smad3* and *Serpinc1*) or 15 μM E2 (*Tnni1*). A new set of mRNA samples was collected at 24 hpf following exposures and mRNA isolation identical to that used for the 0.1 μM microarray analysis. Primers were designed using the NCBI Primer-BLAST tool with default settings, RefSeq mRNA database, and organism = *Danio rerio* (Table 4). Primer pairs were tested prior to the experiment using identical parameters to confirm amplification of the desired product. cDNA was synthesized from 1 μg of RNA using SuperScript® III First Strand Synthesis System (Invitrogen™, Life Technologies Corporation, Carlsbad, CA, USA) according to the standard protocol. The qRT-PCR reaction was prepared using Applied Biosystems Power SYBR® Green PCR Master Mix (Applied Biosystems, Life Technologies Corporation, Carlsbad, CA, USA). The experiment was run using a StepOne™ Instrument (96 wells) and StepOne™ Software v2.2.2 (Applied Biosystems, Life Technologies Corporation, Carlsbad, CA, USA), quantitation-comparative C_T (dd C_T) analysis, and the following program: Holding: 50°C (2 min), 95°C (15 min); Cycling (×40): 95°C (10 s), 60°C (20 s), 72°C (32 s). Biological replicates (N = 3) were run on separate plates. Unpaired t-test ($p < 0.05$) was performed comparing $2^{-\text{dd}C_T}$ values ($\text{d}C_T = C_T \text{ target} - C_T \text{ endogenous control (tbp)}$; $\text{dd}C_T = \text{d}C_T \text{ treatment} - \text{d}C_T \text{ DMSO control}$) of treated versus 0.1% DMSO control samples. All statistics were performed using Prism v6 (GraphPad Software, Inc., La Jolla, CA, USA).

3. Results

3.1. Gene expression profiles following 0.1 versus 80 μM BPA exposure are distinct

Two concentrations of BPA were selected that represented the phenotypes, larval hyperactivity (0.1 μM) or teratogenicity (80 μM) [16]. The lower exposure concentration did not produce any observable defects in 24 or 120 hpf embryos (Figure 1). However, the higher exposure concentration led to lack of pigmentation, ambiguous brain segmentation, and pericardial edema in 24 hpf embryos; and failure to hatch, yolk sac edema, pericardial edema, and craniofacial abnormalities in 120 hpf larvae (Figure 1). Following 24 h exposure to 0.1 or 80 μM BPA, 343 and 352 genes, respectively, of the 38,489 genes on the microarray were significantly different from DMSO control ($p < 0.05$). The 0.1 μM BPA-induced gene expression changes ranged in magnitude from -0.82 to 0.83 log base 2 fold-change (equivalent to 0.57 to 1.77 fold-change) compared to DMSO control, while the 80 μM BPA-induced gene expression changes ranged from -1.02 to 1.23 log2 fold-change (or

0.49 to 2.34 fold-change; Figure 2A). Only 3 of the genes were differentially expressed in the same direction in both datasets: *Tmem206*, *Casp10*, and *C10orf137* (Figure 2B). We annotated 310 and 312 of the 343 and 352 significant differentially expressed 0.1 and 80 μ M-responsive genes, respectively, using either the human ortholog (Entrez gene ID or VegaSeq ID) or the zebrafish gene annotation (Zv8), if the human ID was unavailable. Functional analysis of the annotated gene lists yielded unique predicted canonical pathways and biological functions in the 0.1 versus 80 μ M exposure groups; there were no significant canonical pathways ($-\log(p\text{-value}) > 1.30$; $p < 0.05$; Table 1) or biological functions ($p < 0.01$; Tables S1 and S2) shared between the two BPA concentration groups. The upstream regulator analysis predicted 26 and 25 upstream regulators to be associated with 0.1 and 80 μ M BPA exposure, respectively, based on either a significant p-value ($p < 0.05$) or regulation z-score ($z > 2$ or $z < -2$; Table S3). Only one putative upstream regulator appeared on both BPA exposure lists, HDAC9 (mouse).

3.2. Gene expression profiles following 0.1 versus 15 μ M E2 exposure are distinct

Two concentrations of E2 were included as positive controls reflecting phenotypes similar to those produced by the two BPA exposure concentrations (i.e., larval hyperactivity: 0.1 μ M, or teratogenicity: 15 μ M) [16]. These exposures did not produce observable malformations in 24 hpf embryos or 120 hpf larvae, with the exception that 15 μ M E2 produced subtle yolk sac edema in 120 hpf larvae (Figure 1). Exposure to 0.1 μ M E2 resulted in 375 significant differentially expressed genes ($p < 0.05$; Figure 3A) ranging in magnitude from -0.75 to 1.05 log base 2 fold-change (equivalent to 0.59 to 2.07 fold-change) compared to DMSO control. We annotated 327 of these genes using either the zebrafish gene annotation (Zv8) or the corresponding human ortholog (Entrez ID or VegaSeq ID), and submitted this list for functional analysis. Following 24 h exposure to 15 μ M E2, 457 significant genes were differentially expressed ranging in magnitude from -1.61 to 1.49 log base 2 fold-change (equivalent to 0.33 to 2.81 fold-change), 398 of which were annotated and used in the functional analysis. Only 1 gene, *c10orf137*, from the full, unannotated gene lists was differentially expressed in the same direction in both datasets (Figure 3B). Functional analysis yielded unique predicted canonical pathways and biological functions in the 0.1 versus 15 μ M exposure groups. No significant canonical pathways ($-\log(p\text{-value}) > 1.30$; $p < 0.05$; Table 2) or biological functions ($p < 0.01$; Tables S4 and S5) were shared between the two concentration groups. The upstream regulator analysis predicted 17 and 31 upstream regulators to be associated with 0.1 and 15 μ M E2 exposure, respectively, based on either a significant p-value < 0.05 or regulation z-score > 2 or < -2 (Table S6). No putative upstream regulator appeared on both E2 exposure lists.

3.3. Early embryonic gene expression changes following E2 exposure do not reflect canonical estrogen signaling

Estrogen signaling was not among the significant ($p < 0.05$) canonical pathways (Table 2), and ERs were not among the putative upstream regulators (Table S6) for either the 0.1 or 15 μ M E2 exposure datasets. Although the canonical estrogen signaling pathway was not directly predicted to be impacted by either exposure concentration, two of the predicted upstream regulators associated with the lower concentration dataset, SMARCA4 (BRG1) and AHR, have been implicated in estrogen signaling [24, 25], and 4 of the predicted upstream regulator associated with the higher concentration dataset are regulated by E2: EGR2, STK16, ASB9, and NRF1 [26–29].

3.4. Both 0.1 μ M BPA and 0.1 μ M E2 exposure impact prothrombin activation and coagulation

The 0.1 μ M BPA and E2 exposures were selected because they both lead to larval hyperactivity at 120 hpf following 8–56 hpf exposure [16]. Thus, these comparisons are

based on the similar phenotypic response that they produce rather than anchoring to predictive binding affinity for target receptors. More genes (87) shared significant directional expression changes between the two lower exposures than between the lower versus higher concentration exposures for either compound. Relatively few genes (8 each) comprised each of the 16 and 13 significant ($p < 0.05$) canonical pathways for the 0.1 μM BPA and E2 exposure groups, respectively (Tables 1 and 2). The 3 most significant ($p < 0.001$) canonical pathways for the lower concentration E2 exposure were coagulation system, extrinsic prothrombin activation pathway, and intrinsic prothrombin activation pathway, which included 5, 4, and 4 key genes, respectively (Table 2). The 4 genes occurring in all three pathways that exhibited elevated expression compared to controls were *Serpinc1*, *Proc*, *Fgb*, and *Fgg*. An additional gene, *F2r*, occurring only in the coagulation system pathway, was the only one that exhibited lowered expression compared to controls. These canonical pathways were also among the top 6 significant ($p < 0.05$) canonical pathways predicted for 0.1 μM BPA exposure. All 3 of these pathways comprised three genes: *Serpinc1*, *F13a1*, and *Fgb* (Table 1). We confirmed the elevated expression compared to control for *Serpinc1* following 0.1 μM BPA exposure by qRT-PCR using a new set of samples from embryos exposed as described for the microarray experiment (Table 5). Only 2 upstream regulators, HNF1B ($p = 0.00225$) and TFEC ($p = 0.0233$), were predicted to regulate any of the genes, *Fgb* and *F13a1*, respectively, implicated in prothrombin activation or coagulation following 0.1 μM BPA exposure (Table S3). Similarly, HNF1B ($p = 0.00211$) and STAT3 ($p = 0.0455$) were the only upstream regulators with target genes (HNF1B: *Fgb*; STAT3: *Fgb* and *Fgg*) implicated in prothrombin activation or coagulation, following 0.1 μM E2 exposure (Table S6). Only two significant biological functions were shared between the 0.1 μM E2 versus 0.1 μM BPA exposures, differentiation of kidney cells and size of anterior commissure ($p < 0.01$; Tables S1 and S4).

3.5. 0.1 μM BPA exposure suppresses expression of nervous system development-related genes that are not impacted by 0.1 μM E2 exposure

We hypothesized that nervous system-related genes, signaling pathways, or functions would be associated with the 0.1 μM BPA exposure because this concentration was anchored to a behavioral phenotype that involved larval hyperactivity and adult learning impairments [16]. Consistent with this hypothesis, the canonical pathways comprising the most genes were ERK/MAPK signaling and tight junction signaling, both of which are important in nervous system functioning (Table 1). There were 54 significant ($p < 0.01$) biological functions associated with 0.1 μM BPA exposure (Table S1). Fourteen of these functions described nervous system development or morphology. Development of central nervous system was the ninth most significant function on the list ($p = 0.00247$) and comprised 23 genes: *Apa1*, *Aplp1*, *Arx*, *Asic2*, *Atoh1*, *Cd82*, *Celsr1*, *Faim2*, *Foxb1*, *Gbx2*, *Hgf*, *Ift172*, *Map1b*, *Nlgn4x*, *Otp*, *Plxna4*, *Rfx4*, *Slc1a2*, *Smo*, *Tagln3*, *Tfap2c*, *Trpv1*, and *Tyro3*, which also appeared multiple times under other nervous system-related functions on the list (Table S1). All of these genes exhibited lowered expression compared to controls (Figure 4). Eight of these genes were among the targets for 12 predicted upstream regulators associated with 0.1 μM BPA exposure. The relevant target genes (predicted upstream regulators in parentheses) were *Slc1a2* (MTDH and HOXA13), *Hoxa3* (HOXB3), *Cd82* (TAB2 and APP), *Atoh1* (DAXX and PHF1), *Gbx2* and *Trpv1* (POU4F1 and ISL1), *Hgf* and *Smad3* (SP1), *Hgf* (SIRT1), and *Smad3* (SIM1; Table S3). We confirmed the decreased expression compared to control for *Smad3* following 0.1 μM BPA exposure by qRT-PCR using a new set of samples from embryos exposed as described for the microarray experiment (Table 5).

Although neither CREB nor CBP (CREBBP on IPA-generated networks) were predicted upstream regulators for 0.1 μM BPA exposure, we hypothesized that CREB mediates the suppression of at least some of the 23 nervous system-related genes following 0.1 μM BPA

exposure. The CREB Target Gene Database was used to confirm that 12 of the 29 genes with suppressed expression shown in Figure 3 have predicted CREs on their promoters (Table 3).

As hyperactivity was also the behavioral phenotype to which the 0.1 μM E2 exposure was anchored, we hypothesized that nervous system-related genes, signaling pathways, or functions would also be associated with this exposure concentration. In contrast to the results for 0.1 μM BPA, nervous system development was not directly implicated by any of the 16 significant canonical pathways ($p < 0.05$) or 61 significant ($p < 0.01$) biological functions for 0.1 μM E2 exposure (Tables 2 and S4). However, 8 biological functions (differentiation of sympathetic neuron, proliferation of sympathetic neuron, size of nervous tissue, import of L-glutamic acid, outgrowth of sensory axons, swelling of axons, damage of hippocampal cells, and branching of neurons) collectively comprising 8 genes (*Emx2*, *Hgf*, *Ngf*, *Gm*, *Plxna4*, *Kcnj10*, *Klc1*, and *Slc1a2*) were related to the nervous system (Table S4). Only 3 of these genes (*Hgf*, *Plxna4*, and *Slc1a2*) were among the nervous system development genes impacted by 0.1 μM BPA exposure. Two of these genes, *Hgf* and *Slc1a2*, respectively, were among the targets for 2 predicted upstream regulators, STAT3 and MTDH, following 0.1 μM E2 exposure. Aside from HNF1B, MTDH was the only upstream regulator predicted to regulate both 0.1 μM BPA and 0.1 μM E2 exposures. Additionally, only 9 of the 29 nervous system development-related genes with suppressed expression following 0.1 μM BPA exposure were also suppressed by 0.1 μM E2 exposure (Figure 5). These genes did not reach significance ($p < 0.01$) for enrichment of the biological function, nervous system development, with E2 exposure.

3.6. Multiple canonical pathways and biological functions involved in embryonic development are impacted by both 80 μM BPA and 15 μM E2 exposure

The higher BPA and E2 concentrations both produced teratogenic effects following 8–120 hpf exposure [16]. We therefore hypothesized that impacts on genes governing processes important for proper development would underlie these phenotypes. Consistent with this hypothesis, more genes (189) shared significant directional expression changes between the two teratogenic exposures than between the lower versus higher concentration exposures for either compound. To confirm the expression change of a representative gene from the higher concentration exposures, we selected the gene with the greatest magnitude decrease (0.33) on either microarray, *Thn1*, representing the 15 μM E2 exposure, and measured its expression by qRT-PCR using a new set of samples from embryos exposed as described for the microarray experiment (Table 5).

In addition to shared expression changes among individual genes, there were several canonical pathways and biological functions important to embryonic development that were impacted by exposure to either 80 μM BPA or 15 μM E2. Functional pathway analysis identified adenine and adenosine salvage VI, spliceosomal cycle, and hematopoiesis from multipotent stem cells as canonical pathways impacted by teratogenic concentrations of both BPA and E2 (Tables 1 and 2). The prediction of each of these pathways was based on a single gene, *Adk*, *U2af1*, or *Epo*, respectively, for both exposures. Seventeen significant biological functions were shared between the two higher concentration datasets: cleft palate syndrome, esophageal cancer, differentiation of extraembryonic tissue, polarization of embryonic tissue, abnormal morphology of Purkinje's layer of cerebellum, function of hair cells, abnormal morphology of choroid, sexually transmitted disease, pancreatic tumor, pancreatic cancer, abnormal morphology of glossopharyngeal cranial nerve ganglion, differentiation of beta islet cells, endocrine gland tumor, abnormal morphology of molecular layer of cerebellum, lung cancer, neuroendocrine tumor, and function of neurons. (Tables S2 and S5). Additionally, there were several biological functions related to embryonic development that occurred only on the BPA list, including calcification of osteoblasts,

development of digestive system, development of neural crest, development of external granular layer, neurogenesis of embryonic tissue, synthesis of thromboxane A2, and synthesis of thromboxane B2. Likewise, several biological functions related to embryonic development occurred only on the E2 list, including proliferation of central nervous system cells, proliferation of endothelial progenitor cells, development of trabecular bone, congenital anomaly of musculoskeletal system, and development of hindlimb. Six upstream regulators were predicted to regulate the effects of both 80 μ M BPA and 15 μ M E2 exposure: PIAS3, NFAT (complex), KLF12, SART1, PCBP2, and PCBP1 (Tables S3 and S6).

4. Discussion

Although the molecular events underlying the effects of developmental BPA exposure in animals remain unclear, they appear to involve pathways beyond classical ER signaling. Until molecular modes of action are linked to the phenotypes observed in animal models, it will be difficult to determine whether BPA poses a health risk to developing humans. Microarray analysis is emerging as an important tool for investigating gene expression changes underlying the toxic effects of chemical exposure. Only 2 studies have previously employed this tool to investigate the effects of BPA exposure in zebrafish [15, 30], only one of which was conducted during development. Lam et al. (2011) recently used a 22K microarray to measure whole body mRNA expression in 7 days post fertilization (dpf) larvae following 0–7 dpf daily renewal waterborne BPA exposure [15]. Their functional analysis predicted nervous system development and tight junction signaling, among others, to be impacted by BPA exposure. Our study is the first to assess early embryonic gene expression changes following < 24 hours of BPA exposure. A major objective of this study was to demonstrate that sampling at an early embryonic time point is a useful strategy for identifying gene expression events that precede neurobehavioral or morphological toxicity. However, it is important to recognize some of the limitations in our study design (i.e., a single sampling time point and only two concentrations tested per compound). The hypotheses generated here should therefore serve as a launching point for future investigations focused on the effects of BPA exposure on early embryonic development.

The results described here confirmed our hypothesis that different signaling pathways underlie teratogenic versus non-teratogenic phenotypes and supported our decision to employ phenotypic anchoring for comparing the effects of different chemicals. By selecting an early time point, we captured gene expression changes that are presumably at the beginning of a cascade of signaling miscues leading to the observed phenotypes. Sampling at a time point that precedes an observable phenotype minimizes potential interference of secondary effects that could confound identification of BPA's primary target molecules. The 24 hpf time point preceded evidence of toxicity for all concentrations tested, except 80 μ M BPA. It is therefore possible that the gene expression events measured for the 80 μ M BPA exposure group were secondary effects located farther down the signaling cascade. Inclusion of additional exposure concentrations followed by functional analysis to identify groups of genes and signaling pathways impacted by a range of BPA concentrations (i.e., a concentration-response curve with gene expression as the response) would help identify gene expression changes associated only with the higher, acutely toxic exposure concentrations that could be due to secondary effects.

Because embryogenesis is a time of rapid development and dynamic gene expression changes, our selection of a single time point provided only a snapshot of gene activity at this time. Thus, although the results of the microarray and pathway analyses suggested that certain genes and signaling pathways are not impacted by BPA and/or E2 exposure at 24 hpf, the same potential targets could be affected at other times during development. For

example, an interesting outcome of selecting the 24 hpf tissue collection time point was the conspicuous absence of estrogen signaling from the significant canonical pathways and absence of ERs from the upstream regulator analysis for both E2 exposure groups. This result highlighted the nuances of using E2 as a positive control in 24 hpf embryos and was consistent with related observations in previous zebrafish studies [31, 32]. Although ERs are present at this age, ER mRNA rises substantially shortly after 24 hpf [33]. Therefore, the 24 hpf time point may be slightly too early to detect ER activation. Future studies designed to more fully characterize the effects of BPA versus E2 exposure throughout embryonic development should therefore include additional sampling time points.

The primary reason for including E2 as a positive control was to investigate whether BPA exerts effects similar to those caused by E2 at the molecular or functional level. Because unidentified differences in absorption and target receptor binding affinities complicate the identification of analogous BPA and E2 exposure concentrations, we anchored the concentrations to similar phenotypes (i.e., yolk sac edema) in order to compare global gene expression changes following BPA versus E2 exposure. Although this approach proved useful for identifying some similar effects underlying the shared phenotypes, it is also important to note that both larval hyperactivity and teratogenic effects such as yolk sac edema are common responses that have been observed following embryonic zebrafish exposure to a wide array of chemicals with distinct modes of action (e.g., dioxin [34]). Importantly, the higher BPA concentration was also associated with acute toxicity present both at the sampling time point (e.g., pericardial edema, reduced pigmentation, and brain structural malformations) and at 5 dpf (e.g., failure to hatch, severe yolk sac and pericardial edema, and craniofacial malformations). Thus, although the higher E2 and BPA exposures were anchored by the shared phenotype, yolk sac edema, the presence of additional malformations in the BPA-exposed group could confound the interpretation of results. Namely, it is difficult to distinguish whether the observed gene expression changes were primary responses to BPA exposure or secondary responses located farther down the putative signaling cascade initiated by BPA exposure. Future inclusion of additional exposure concentrations to obtain gene expression concentration-response curves for both BPA and E2 would aid in identifying the signaling events that are associated only with the yolk sac edema common to both BPA and E2 exposure. The 0.1 μM exposure for both BPA and E2 elicited a hyperactive phenotype in the absence of visible morphological defects at 5 dpf following 8 – 56 hpf exposure [16]. Although hyperactivity is a common response that could be a result of impacts on a number of target organ systems, we hypothesized that it was a result of impaired nervous system development. Interestingly, although nervous system development was perturbed by 0.1 μM BPA exposure, it was not identified as a significant function impacted by 0.1 μM E2 exposure.

More striking was the appearance of extrinsic/intrinsic prothrombin activation among the top significant canonical pathways for both 0.1 μM BPA and 0.1 μM E2 exposures. There is evidence that perturbation of thrombin signaling may affect nervous system development and function. Prothrombin is expressed in the developing brain [35], and thrombin inhibited neurite outgrowth in a rat embryonic dorsal root ganglion model [36]. Additionally, a microarray study using RNA collected from embryonic zebrafish following antisense oligonucleotide knockdown of prothrombin identified a set of target genes that are expressed in the developing brain (e.g., *Sox21a*), suggesting that thrombin has a role in vertebrate nervous system development [37]. Therefore, while impacts on prothrombin activation following 0.1 μM BPA or E2 exposure may be insufficient to cause overt impairment of the coagulation system (i.e., no hemorrhage, edema, or circulatory problems were previously noted in exposed embryos up to 5 dpf), these effects may be sufficient to impair neuronal development leading to the hyperactive phenotype observed at 5 dpf (BPA and E2) or the learning deficits observed in adult zebrafish following embryonic BPA exposure [16].

More direct support of our hypothesis was the identification of nervous system development among the significant biological functions predicted to be impacted by 0.1 μM BPA exposure. Notably, all of the 23 genes comprising this function, in addition to 5 genes selected from the IPA-generated interaction networks, exhibited lowered expression compared to controls following 0.1 μM BPA exposure. This common feature suggested the role of a mechanism specialized in regulating expression of multiple target genes, such as histone acetylation. CREB binding protein (CREBBP or CBP) appeared as a hub on the top network generated by IPA for the 0.1 μM BPA exposure (data not shown). CBP is an acetyltransferase that can function alone or in a coactivator complex. CBP expression was lowered following 0.1 μM BPA exposure, hypothetically leading to a reduction in CBP-mediated acetylation and a decrease in transcription of target genes, which we observed. CBP's primary role is as a coactivator of the cyclic AMP response element binding protein (CREB) family of transcription activators. Importantly, CREB not only has a regulatory role in neurons that involves ERK/MAPK signaling [38], but it is also involved in neuron proliferation and brain patterning in developing zebrafish [39]. Furthermore, BPA activates CREB through a membrane-bound estrogen receptor in mouse islet cells [40]. We used the CREB target gene database (<http://natural.salk.edu/CREB/>) to determine whether the nervous system-related genes on our list are predicted to have cyclic AMP response elements (CREs) on their promoters [23]. Compellingly, 40% of the suppressed genes have CREs on their promoters (Table 3). Furthermore, a microRNA regulated by CREB and implicated in neuronal plasticity, miR-132 [41], targets 3 of the genes on our list. Interestingly, HNF1, an upstream regulator putatively activated by 0.1 μM BPA exposure, is a coactivator of CBP [42].

This study serves as a launching point for future studies. Namely, in order to capture gene expression events representing the rapid and dynamic period of organogenesis, it would be useful to include multiple sampling time points (e.g., 12, 18, 24, and 30 hpf). Future studies aimed at obtaining a gene expression concentration-response curve should include concentrations between those tested here (e.g., 1 and 10 μM). Functional analysis of the 80 μM BPA-responsive data set yielded few results that obviously suggested secondary effects. For example, inflammation or oxidative stress did not appear on the biological functions list (Table S2). However, a function that could indicate generalized toxicity, degradation of cells, appeared on this list. Inclusion of additional sampling concentrations and time points in follow-up studies will aid in distinguishing which signaling events are more likely associated with BPA's primary versus secondary effects. RNA sequencing may be a preferable method for global gene expression analysis because this technology is not limited to the genes on a given microarray and deeper sequencing provides greater statistical power to detect modest gene expression changes [43].

5. Conclusion

Taken together, the findings of this study demonstrated that low fold-change expression data is useful for hypothesis generation when phenotype-anchored effects on groups of genes (i.e., a pathway-based approach) are considered. These data showed that 24 hpf gene expression changes and signaling pathways are differentially impacted by non-teratogenic versus teratogenic exposure concentrations of BPA and E2, respectively. Additionally, developmental exposure to both 0.1 μM BPA and 0.1 μM E2, concentrations previously associated with larval behavioral impairments, impacted key genes involved in prothrombin signaling, while only the 0.1 μM BPA exposure caused a general suppression of genes required for proper nervous system development. While we chose to focus on nervous system-related genes in an effort to identify genes mediating the behavioral phenotype observed following 0.1 μM BPA exposure, multiple systems were impacted by developmental BPA exposure.

Supplementary Material

Refer to Web version on PubMed Central for supplementary material.

Acknowledgments

We thank Margaret Corvi for sample collection assistance; Jane La Du for imaging assistance; Eric Johnson, Cari Buchner, Carrie Barton, and Greg Gonnerman for providing fish husbandry; and Siba Das, Sean Bugel, and Fred Tilton for critical review of the manuscript. This work was supported by NIH grants T32 ES7060, P30 ES000210 and R21 ES018970 and a United States Environmental Protection Agency (EPA) Science to Achieve Results (STAR) Graduate Fellowship (KSS). The Pacific Northwest National Laboratory is a multi-program national laboratory operated by Battelle Memorial Institute for the DOE under contract number DE-AC05-76RLO1830. The funding sources were not involved in any part of the design, execution, analysis, or publication of this study. EPA has not officially endorsed this publication and the views expressed herein do not necessarily reflect the views of the EPA.

References

1. Teeguarden JG, Calafat AM, Ye X, Doerge DR, Churchwell MI, Gunawan R, et al. Twenty-four hour human urine and serum profiles of bisphenol a during high-dietary exposure. *Toxicological sciences : an official journal of the Society of Toxicology*. 2011; 123:48–57. [PubMed: 21705716]
2. Vandenberg LN, Chahoud I, Heindel JJ, Padmanabhan V, Paumgarten FJ, Schoenfelder G. Urinary, circulating, and tissue biomonitoring studies indicate widespread exposure to bisphenol A. *Environmental health perspectives*. 2010; 118:1055–70. [PubMed: 20338858]
3. Melzer D, Rice NE, Lewis C, Henley WE, Galloway TS. Association of urinary bisphenol a concentration with heart disease: evidence from NHANES 2003/06. *PloS one*. 2010; 5:e8673. [PubMed: 20084273]
4. Trasande L, Attina TM, Blustein J. Association between urinary bisphenol A concentration and obesity prevalence in children and adolescents. *JAMA : the journal of the American Medical Association*. 2012; 308:1113–21. [PubMed: 22990270]
5. Rubin BS. Bisphenol A: an endocrine disruptor with widespread exposure and multiple effects. *The Journal of steroid biochemistry and molecular biology*. 2011; 127:27–34. [PubMed: 21605673]
6. Shelby MD. NTP-CERHR monograph on the potential human reproductive and developmental effects of bisphenol A. *Ntp Cerhr Mon*. 2008:v, vii–ix, 1–64. passim. [PubMed: 19407859]
7. Perera F, Vishnevetsky J, Herbstman JB, Calafat AM, Xiong W, Rauh V, et al. Prenatal bisphenol a exposure and child behavior in an inner-city cohort. *Environmental health perspectives*. 2012; 120:1190–4. [PubMed: 22543054]
8. Braun JM, Kalkbrenner AE, Calafat AM, Yolton K, Ye X, Dietrich KN, et al. Impact of early-life bisphenol A exposure on behavior and executive function in children. *Pediatrics*. 2011; 128:873–82. [PubMed: 22025598]
9. Thomas P, Dong J. Binding and activation of the seven-transmembrane estrogen receptor GPR30 by environmental estrogens: a potential novel mechanism of endocrine disruption. *The Journal of steroid biochemistry and molecular biology*. 2006; 102:175–9. [PubMed: 17088055]
10. Takayanagi S, Tokunaga T, Liu X, Okada H, Matsushima A, Shimohigashi Y. Endocrine disruptor bisphenol A strongly binds to human estrogen-related receptor gamma (ERRgamma) with high constitutive activity. *Toxicology letters*. 2006; 167:95–105. [PubMed: 17049190]
11. Imanishi S, Manabe N, Nishizawa H, Morita M, Sugimoto M, Iwahori M, et al. Effects of oral exposure of bisphenol A on mRNA expression of nuclear receptors in murine placenta assessed by DNA microarray. *The Journal of reproduction and development*. 2003; 49:329–36. [PubMed: 14967926]
12. Moral R, Wang R, Russo IH, Lamartiniere CA, Pereira J, Russo J. Effect of prenatal exposure to the endocrine disruptor bisphenol A on mammary gland morphology and gene expression signature. *The Journal of endocrinology*. 2008; 196:101–12. [PubMed: 18180321]
13. Naciff JM, Jump ML, Torontali SM, Carr GJ, Tiesman JP, Overmann GJ, et al. Gene expression profile induced by 17alpha-ethynyl estradiol, bisphenol A, and genistein in the developing female

- reproductive system of the rat. *Toxicological sciences : an official journal of the Society of Toxicology*. 2002; 68:184–99. [PubMed: 12075121]
14. Heimeier RA, Das B, Buchholz DR, Shi YB. The xenoestrogen bisphenol A inhibits postembryonic vertebrate development by antagonizing gene regulation by thyroid hormone. *Endocrinology*. 2009; 150:2964–73. [PubMed: 19228888]
 15. Lam SH, Hlaing MM, Zhang X, Yan C, Duan Z, Zhu L, et al. Toxicogenomic and phenotypic analyses of bisphenol-A early-life exposure toxicity in zebrafish. *PloS one*. 2011; 6:e28273. [PubMed: 22194820]
 16. Saili KS, Corvi MM, Weber DN, Patel AU, Das SR, Przybyla J, et al. Neurodevelopmental low-dose bisphenol A exposure leads to early life-stage hyperactivity and learning deficits in adult zebrafish. *Toxicology*. 2012; 291:83–92. [PubMed: 22108044]
 17. Kimmel CB, Ballard WW, Kimmel SR, Ullmann B, Schilling TF. Stages of embryonic development of the zebrafish. *Developmental dynamics : an official publication of the American Association of Anatomists*. 1995; 203:253–310. [PubMed: 8589427]
 18. Bolstad BM, Irizarry RA, Astrand M, Speed TP. A comparison of normalization methods for high density oligonucleotide array data based on variance and bias. *Bioinformatics*. 2003; 19:185–93. [PubMed: 12538238]
 19. Edgar R, Domrachev M, Lash AE. Gene Expression Omnibus: NCBI gene expression and hybridization array data repository. *Nucleic acids research*. 2002; 30:207–10. [PubMed: 11752295]
 20. Saeed AI, Sharov V, White J, Li J, Liang W, Bhagabati N, et al. TM4: a free, open-source system for microarray data management and analysis. *BioTechniques*. 2003; 34:374–8. [PubMed: 12613259]
 21. Shah AR, Singhal M, Klicker KR, Stephan EG, Wiley HS, Waters KM. Enabling high-throughput data management for systems biology: the Bioinformatics Resource Manager. *Bioinformatics*. 2007; 23:906–9. [PubMed: 17324940]
 22. Huang da W, Sherman BT, Lempicki RA. Systematic and integrative analysis of large gene lists using DAVID bioinformatics resources. *Nature protocols*. 2009; 4:44–57.
 23. Zhang X, Odom DT, Koo SH, Conkright MD, Canettieri G, Best J, et al. Genome-wide analysis of cAMP-response element binding protein occupancy, phosphorylation, and target gene activation in human tissues. *Proceedings of the National Academy of Sciences of the United States of America*. 2005; 102:4459–64. [PubMed: 15753290]
 24. Ichinose H, Garnier JM, Chambon P, Losson R. Ligand-dependent interaction between the estrogen receptor and the human homologues of SWI2/SNF2. *Gene*. 1997; 188:95–100. [PubMed: 9099865]
 25. Kharat I, Saatcioglu F. Antiestrogenic effects of 2,3,7,8-tetrachlorodibenzo-p-dioxin are mediated by direct transcriptional interference with the liganded estrogen receptor. Cross-talk between aryl hydrocarbon- and estrogen-mediated signaling. *The Journal of biological chemistry*. 1996; 271:10533–7. [PubMed: 8631852]
 26. Frasor J, Danes JM, Komm B, Chang KC, Lyttle CR, Katzenellenbogen BS. Profiling of estrogen up- and down-regulated gene expression in human breast cancer cells: insights into gene networks and pathways underlying estrogenic control of proliferation and cell phenotype. *Endocrinology*. 2003; 144:4562–74. [PubMed: 12959972]
 27. Frasor J, Stossi F, Danes JM, Komm B, Lyttle CR, Katzenellenbogen BS. Selective estrogen receptor modulators: discrimination of agonistic versus antagonistic activities by gene expression profiling in breast cancer cells. *Cancer research*. 2004; 64:1522–33. [PubMed: 14973112]
 28. Ivanga M, Labrie Y, Calvo E, Belleau P, Martel C, Luu-The V, et al. Temporal analysis of E2 transcriptional induction of PTP and MKP and downregulation of IGF-I pathway key components in the mouse uterus. *Physiological genomics*. 2007; 29:13–23. [PubMed: 17361005]
 29. Pedram A, Razandi M, Aitkenhead M, Hughes CC, Levin ER. Integration of the non-genomic and genomic actions of estrogen. Membrane-initiated signaling by steroid to transcription and cell biology. *The Journal of biological chemistry*. 2002; 277:50768–75. [PubMed: 12372818]

30. Kausch U, Alberti M, Haindl S, Budczies J, Hock B. Biomarkers for exposure to estrogenic compounds: gene expression analysis in zebrafish (*Danio rerio*). *Environmental toxicology*. 2008; 23:15–24. [PubMed: 18214933]
31. Brion F, Le Page Y, Piccini B, Cardoso O, Tong SK, Chung BC, et al. Screening estrogenic activities of chemicals or mixtures in vivo using transgenic (cyp19a1b-GFP) zebrafish embryos. *PloS one*. 2012; 7:e36069. [PubMed: 22586461]
32. Tong SK, Mouriec K, Kuo MW, Pellegrini E, Gueguen MM, Brion F, et al. A cyp19a1b-gfp (aromatase B) transgenic zebrafish line that expresses GFP in radial glial cells. *Genesis*. 2009; 47:67–73. [PubMed: 19101983]
33. Tingaud-Sequeira A, Andre M, Forgue J, Barthe C, Babin PJ. Expression patterns of three estrogen receptor genes during zebrafish (*Danio rerio*) development: evidence for high expression in neuromasts. *Gene expression patterns : GEP*. 2004; 4:561–8. [PubMed: 15261834]
34. Mathew LK, Andreasen EA, Tanguay RL. Aryl hydrocarbon receptor activation inhibits regenerative growth. *Molecular pharmacology*. 2006; 69:257–65. [PubMed: 16214955]
35. Dihanich M, Kaser M, Reinhard E, Cunningham D, Monard D. Prothrombin mRNA is expressed by cells of the nervous system. *Neuron*. 1991; 6:575–81. [PubMed: 2015093]
36. Gill JS, Pitts K, Rusnak FM, Owen WG, Windebank AJ. Thrombin induced inhibition of neurite outgrowth from dorsal root ganglion neurons. *Brain research*. 1998; 797:321–7. [PubMed: 9666159]
37. Day KR, Jagadeeswaran P. Microarray analysis of prothrombin knockdown in zebrafish. *Blood cells, molecules & diseases*. 2009; 43:202–10.
38. Yang BH, Son H, Kim SH, Nam JH, Choi JH, Lee JS. Phosphorylation of ERK and CREB in cultured hippocampal neurons after haloperidol and risperidone administration. *Psychiatry and clinical neurosciences*. 2004; 58:262–7. [PubMed: 15149291]
39. Dworkin S, Heath JK, deJong-Curtain TA, Hogan BM, Lieschke GJ, Malaterre J, et al. CREB activity modulates neural cell proliferation, midbrain-hindbrain organization and patterning in zebrafish. *Developmental biology*. 2007; 307:127–41. [PubMed: 17531969]
40. Quesada I, Fuentes E, Viso-Leon MC, Soria B, Ripoll C, Nadal A. Low doses of the endocrine disruptor bisphenol-A and the native hormone 17beta-estradiol rapidly activate transcription factor CREB. *FASEB journal : official publication of the Federation of American Societies for Experimental Biology*. 2002; 16:1671–3. [PubMed: 12207000]
41. Nudelman AS, DiRocco DP, Lambert TJ, Garelick MG, Le J, Nathanson NM, et al. Neuronal activity rapidly induces transcription of the CREB-regulated microRNA-132, in vivo. *Hippocampus*. 2010; 20:492–8. [PubMed: 19557767]
42. Soutoglou E, Papafotiou G, Katrakili N, Talianidis I. Transcriptional activation by hepatocyte nuclear factor-1 requires synergism between multiple coactivator proteins. *The Journal of biological chemistry*. 2000; 275:12515–20. [PubMed: 10777539]
43. Gomez G, Lee JH, Veldman MB, Lu J, Xiao X, Lin S. Identification of vascular and hematopoietic genes downstream of etsrp by deep sequencing in zebrafish. *PloS one*. 2012; 7:e31658. [PubMed: 22438865]

Highlights

- Gene expression changes are distinct following 0.1 μM versus 80 μM BPA exposure.
- Gene expression changes are distinct following 0.1 μM versus 15 μM E2 exposure.
- Both 0.1 μM bisphenol A and 0.1 μM E2 exposures impact prothrombin signaling.
- 0.1 μM bisphenol A exposure suppresses nervous system development-related genes.

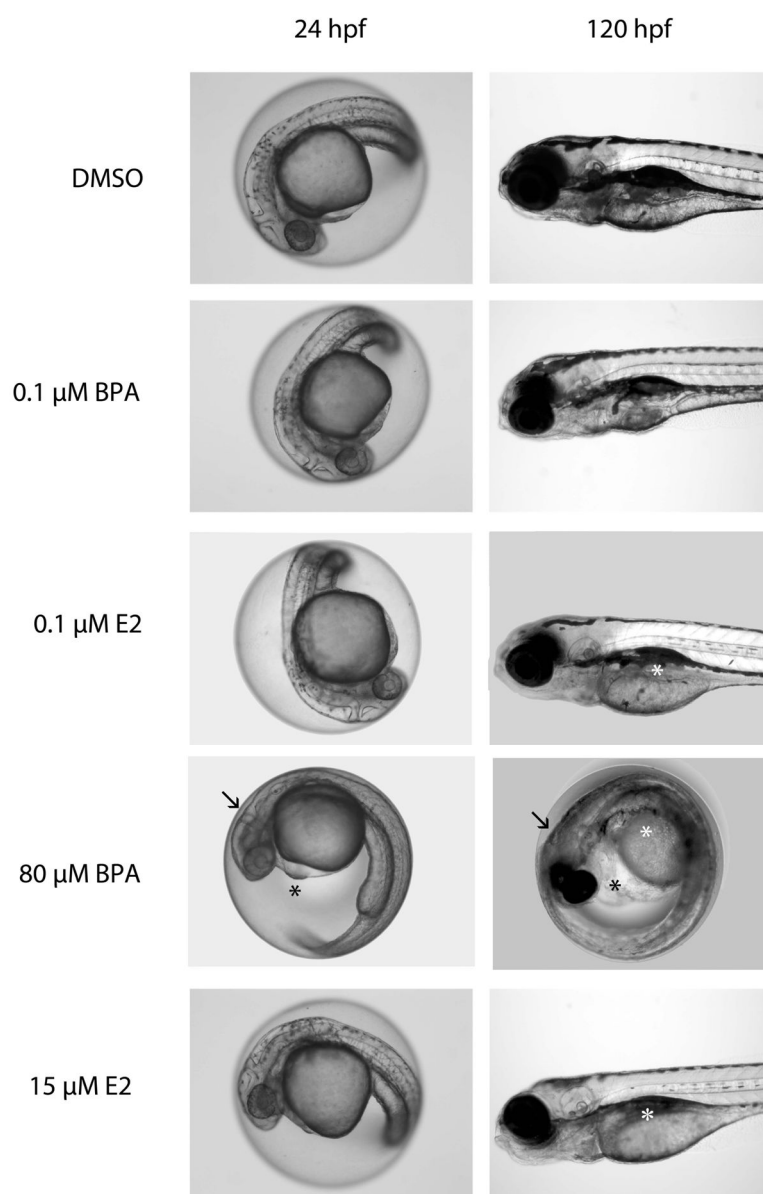


Figure 1. Representative images of 24 hpf and 120 hpf embryos following exposure to control, BPA, or E2

At 24 hpf (the microarray sampling time point), all embryos appeared similar to controls, with the exception that the 80 μM BPA – exposed embryos exhibited moderate pericardial edema (black asterisk) and ambiguous boundaries in the brain region (arrow). At 120 hpf, all larvae appeared similar to controls, with the exception that embryos exposed to both concentrations of E2 exhibited very moderate yolk sac edema (white asterisks), while the 80 μM BPA – exposed larvae failed to hatch and exhibited lack of pigmentation, severe yolk sac edema (white asterisk), severe pericardial edema (black asterisk), and craniofacial abnormalities (arrow).

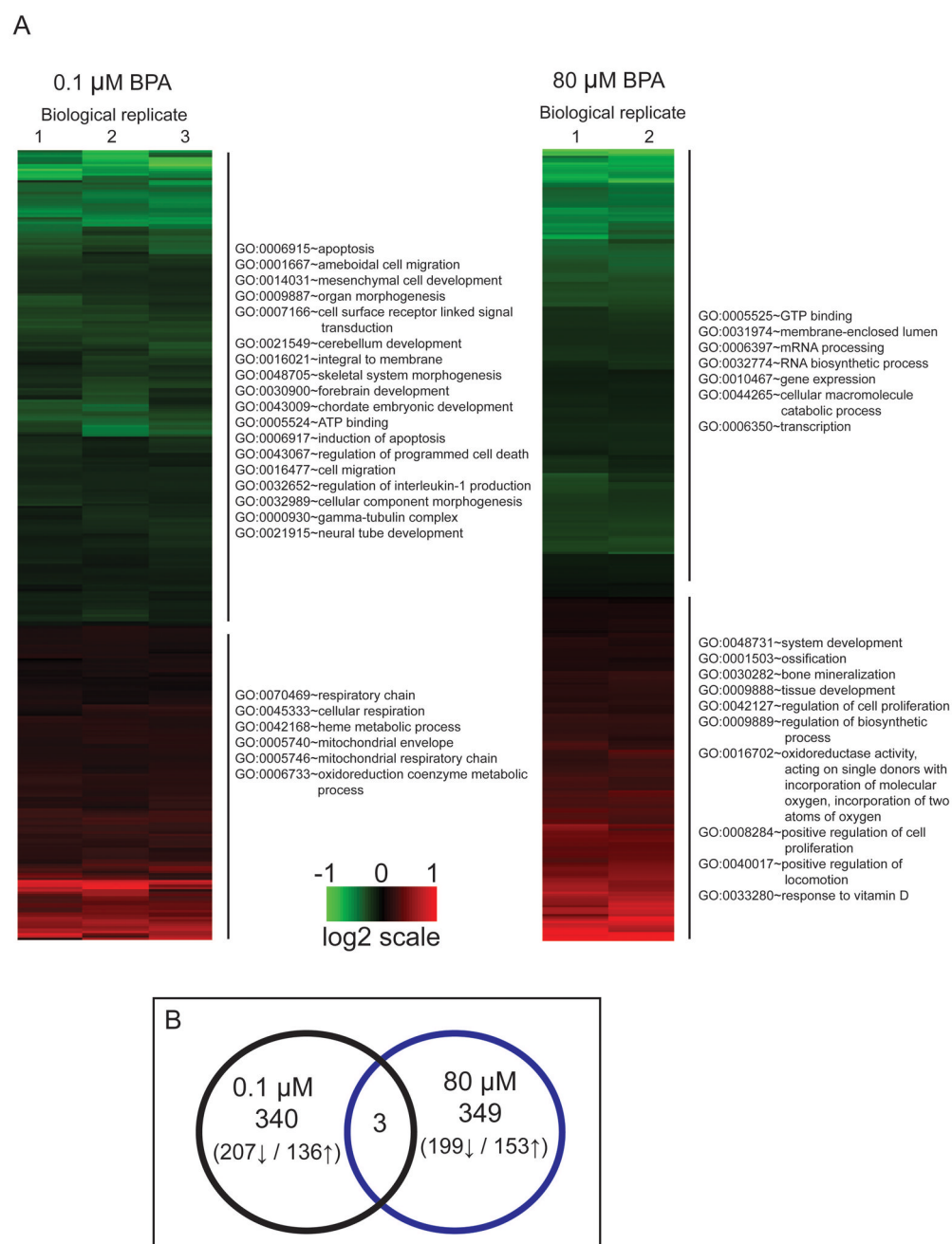


Figure 2. Representation of significant genes differentially expressed following 8 – 24 hpf exposure to BPA

A) Bidirectional hierarchical clustering showing genes differentially expressed compared to stage-matched controls (0.1% DMSO) following BPA exposure (green = lowered expression; red = increased expression). Gene lists derived by conducting a one-way ANOVA, no FDR applied, no fold expression change cutoff, $N = 3$ (low), $N = 2$ (high), $p < 0.05$. Scale is log base 2 of expression values. Annotation: GO terms ($p < 0.05$) representing significant clusters by DAVID functional clustering analysis arranged by enrichment score.

B) Venn diagrams depicting relationship between 0.1 versus 80 μM BPA expression

profiles. Only 3 genes were differentially expressed in the same direction for both lower and higher concentration exposure to BPA. Numbers include unannotated genes.

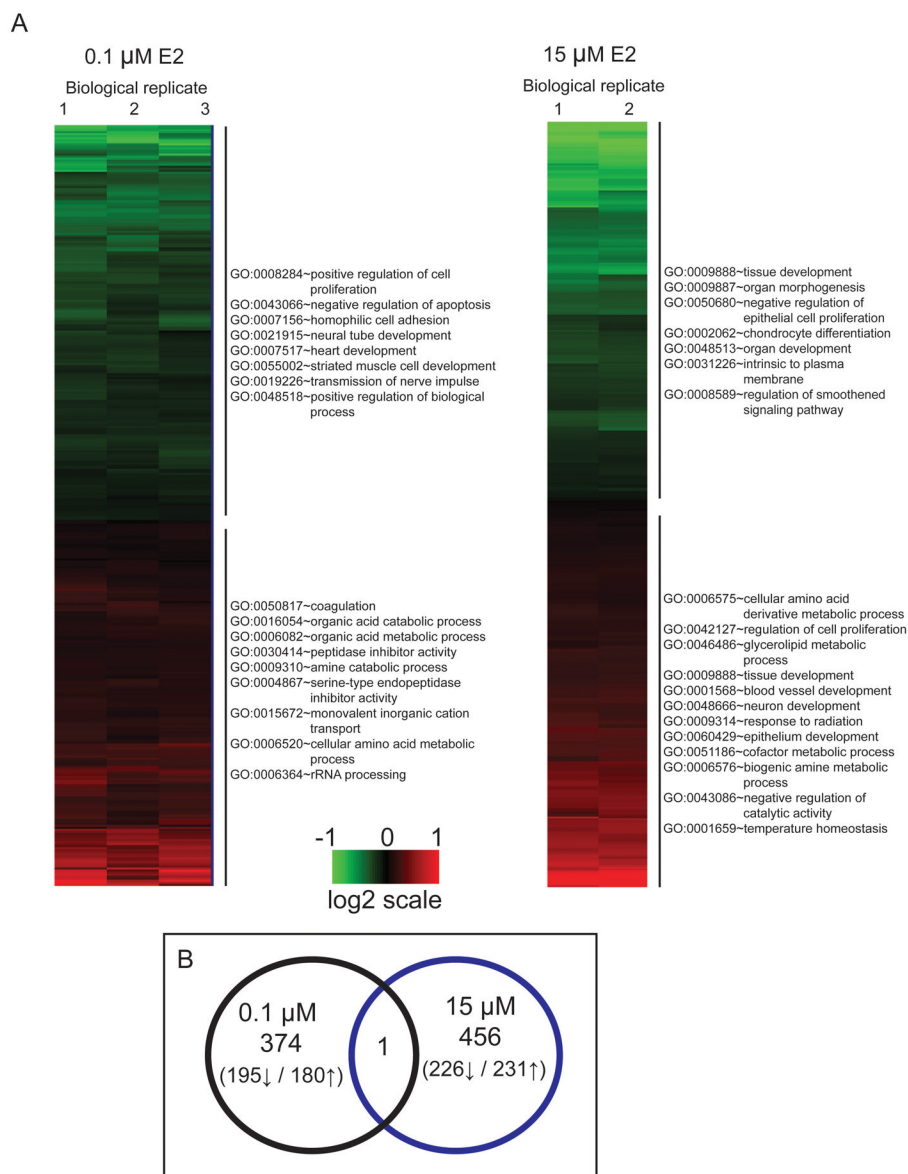


Figure 3. Representation of significant genes differentially expressed following 8 – 24 hpf exposure to E2

A) Bidirectional hierarchical clustering showing genes differentially expressed compared to stage-matched controls (0.1% DMSO) following E2 exposure (green = lowered expression; red = increased expression). Gene lists derived by conducting a one-way ANOVA, no FDR applied, no fold expression change cutoff, N = 3 (low), N = 2 (high), $p < 0.05$. Scale is log base 2 of expression values. Annotation: GO terms ($p < 0.05$) representing significant clusters by DAVID functional clustering analysis arranged by enrichment score. B) Venn diagrams depicting relationship between 0.1 versus 15 μ M E2 expression profiles. Only 1 gene was differentially expressed in the same direction for both lower and higher concentration exposure to E2. Numbers include unannotated genes.

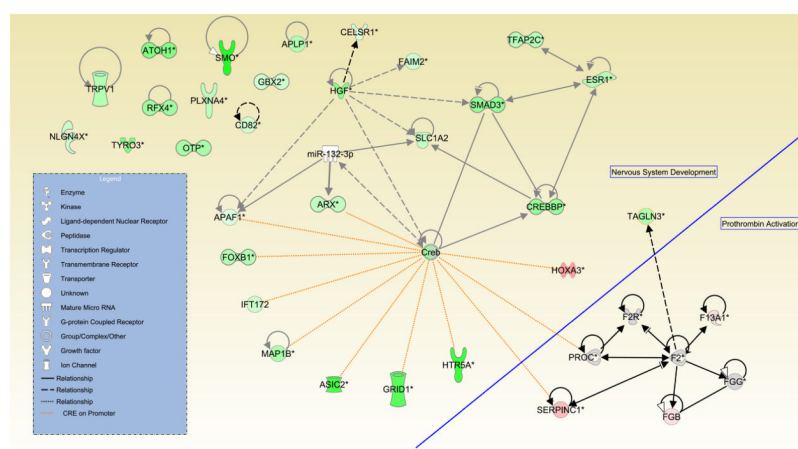


Figure 4. Network showing putative CREB-mediated regulation of genes impacted by 0.1 μ M BPA exposure

Genes included in the IPA-generated network were predicted by core analysis to be important in prothrombin activation (right) or nervous system development and function. Genes with CREs on their promoters are listed in Table 3 (relationships manually added based on the CREB Target Gene Database predictions are indicated by dotted orange lines). Solid lines represent direct interactions; dotted lines represent indirect interactions. Arrows are IPA-generated and do not necessarily indicate activation. Green molecules: lowered expression compared to controls, red molecules: elevated expression compared to controls, grey molecules: expression did not change upon BPA exposure, white molecule: not included on the microarray. Asterisk after a symbol depicts duplicate identifiers for the same gene.

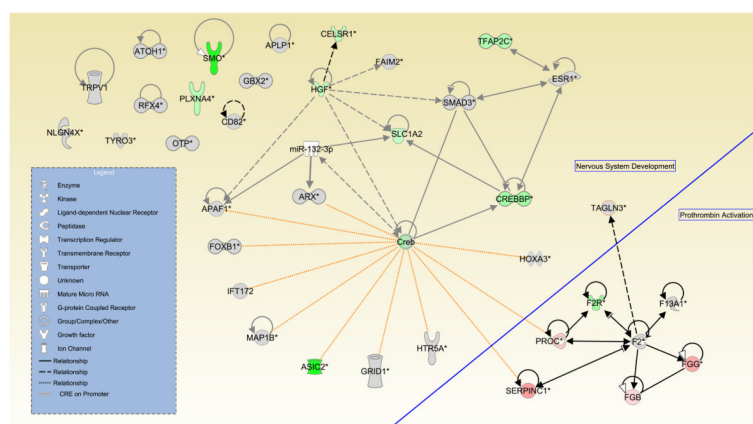


Figure 5. Network showing putative CREB-mediated regulation of genes impacted by 0.1 μ M E2 exposure

IPA-generated network shows 0.1 μ M E2 expression values overlaying the putative CREB-mediated regulatory network comprising genes important in prothrombin activation (right) or nervous system development and function impacted by 0.1 μ M BPA exposure (see Figure 3). Solid lines represent direct interactions; dotted lines represent indirect interactions.

Arrows are IPA-generated and do not necessarily indicate activation. Green molecules: lowered expression compared to controls, red molecules: elevated expression compared to controls, grey molecules: expression did not change upon E2 exposure, white molecule: not included on the microarray. Asterisk after a symbol depicts duplicate identifiers for the same gene.

Table 1

Significant ($p < 0.05$) canonical pathways predicted by Ingenuity Pathway Analysis using annotated human orthologs of zebrafish genes differentially expressed following 8–24 hpf BPA exposure.

BPA Conc.	Ingenuity Canonical Pathways	$-\log(p\text{-value})$	Molecules
0.1 μM	Uracil Degradation II (Reductive)	2.85E00	CRMP1,DPYD
	Thymine Degradation	2.85E00	CRMP1,DPYD
	Extrinsic Prothrombin Activation Pathway	2.6E00	SERPINC1,F13A1,FGB
	Intrinsic Prothrombin Activation Pathway	2.18E00	SERPINC1,F13A1,FGB
	Lymphotoxin β Receptor Signaling	1.96E00	TRAF3,CYCS,CREBBP,APAF1
	Coagulation System	1.82E00	SERPINC1,F13A1,FGB
	ERK/MAPK Signaling	1.78E00	HSPB3,PRKCI,CREBBP,PPP2R5B,PP2R2C,TLN1,ESR1,DUSP2
	Role of RIG1-like Receptors in Antiviral Innate Immunity	1.78E00	TRAF3,CREBBP,CASP10
	Tight Junction Signaling	1.73E00	PRKCI,PPP2R5B,PPP2R2C,CPSF3,M YH7,SAFB,ACTG1
	TWEAK Signaling	1.73E00	TRAF3,CYCS,APAF1
	Death Receptor Signaling	1.69E00	HSPB3,CYCS,APAF1,CASP10
	Role of PKR in Interferon Induction and Antiviral Response	1.53E00	TRAF3,CYCS,APAF1
	Granzyme B Signaling	1.5E00	CYCS,APAF1
	2-ketoglutarate Dehydrogenase Complex	1.36E00	OGDH
	Mechanisms of Viral Exit from Host Cells	1.36E00	PRKCI,CHMP4B,ACTG1
	Ceramide Signaling	1.35E00	S1PR3,CYCS,PPP2R5B,PPP2R2C
80 μM	MIF-mediated Glucocorticoid Regulation	2.23E00	PLA2G4A,RELA,PTGS2
	MIF Regulation of Innate Immunity	1.88E00	PLA2G4A,RELA,PTGS2
	Caveolar-mediated Endocytosis Signaling	1.87E00	ARCN1,INSR,ITGB8,PTRF
	Adenine and Adenosine Salvage VI	1.75E00	ADK
	TREM1 Signaling	1.65E00	RELA,GRB2,Tlr12
	Endothelin-1 Signaling	1.56E00	ADCY9,PLA2G4A,GRB2,PTGS2,PLC D4,CASP10
	PPAR Signaling	1.53E00	RELA,GRB2,PTGS2,INSR
	Spliceosomal Cycle	1.45E00	U2AF1
	Hematopoiesis from Multipotent Stem Cells	1.45E00	EPO
	Maturity Onset Diabetes of Young (MODY) Signaling	1.35E00	CACNA1D,INSR

Table 2

Significant ($p < 0.05$) canonical pathways predicted by Ingenuity Pathway Analysis using annotated human orthologs of zebrafish genes differentially expressed following 8–24 hpf E2 exposure.

E2 Conc.	Ingenuity Canonical Pathways	$-\log(p\text{-value})$	Molecules
0.1 μM	Extrinsic Prothrombin Activation Pathway	3.96E+00	SERPINC1,PROC,FGB,FGG
	Coagulation System	3.95E+00	SERPINC1,F2R,PROC,FGB,FGG
	Intrinsic Prothrombin Activation Pathway	3.36E+00	SERPINC1,PROC,FGB,FGG
	Glycine Betaine Degradation	2.39E+00	SARDH,DMGDH
	Ketolysis	2.22E+00	BDH2 (includes EG:295458),OXCT1
	Xanthine and Xanthosine Salvage	1.68E+00	PNP
	Calcium-induced T Lymphocyte Apoptosis	1.45E+00	ATP2A1,ITPR3,NR4A1
	Guanine and Guanosine Salvage I	1.39E+00	PNP
	Tetrahydrobiopterin Biosynthesis I	1.39E+00	GCH1
	Purine Ribonucleosides Degradation to Ribose-1-phosphate	1.39E+00	PNP
	Fatty Acid Biosynthesis Initiation II	1.39E+00	OXSM
	Adenine and Adenosine Salvage I	1.39E+00	PNP
	Tetrahydrobiopterin Biosynthesis II	1.39E+00	GCH1
15 μM	Methylmalonyl Pathway	2.46E+00	PCCA,MCEE
	2-oxobutanoate Degradation I	2.25E+00	PCCA,MCEE
	Basal Cell Carcinoma Signaling	1.73E+00	PTCH1,WNT16,WNT4,HHIP,PTC H2
	Sonic Hedgehog Signaling	1.65E+00	PTCH1,HHIP,PTCH2
	L-cysteine Degradation II	1.61E+00	CTH
	Adenine and Adenosine Salvage VI	1.61E+00	ADK
	Spliceosomal Cycle	1.32E+00	U2AF1
	Hematopoiesis from Multipotent Stem Cells	1.32E+00	EPO
	Cysteine Biosynthesis/Homocysteine Degradation	1.32E+00	CTH
	Role of PI3K/AKT Signaling in the Pathogenesis of Influenza	1.22E+00	RELA,CCR5,CRKL

Table 3

CREB Target Gene Database (<http://natural.salk.edu/CREB/>) prediction of cAMP response elements (CREs) occurring on promoters of nervous system-associated or prothrombin activation- associated genes shown in Figures 4 and 5.

CREB Target Prediction	Protein Symbol	Basis of Inclusion in Figure 3	CRE Description
Predicted CREB target	ASIC2	Development of central nervous system (Table S1)	cre-noTATA
	APAF1	Development of central nervous system (Table S1)	cre-noTATA
	ARX	Development of central nervous system (Table S1)	cre-noTATA
	CREB	Manually added from IPA-generated networks	cre-TATA
	CREBBP	Manually added from IPA-generated networks	cre-noTATA
	FOXB1	Development of central nervous system (Table S1)	cre-TATA
	GRID1	Manually added from IPA-generated networks	cre-noTATA
	HGF	Development of central nervous system (Table S1)	cre-TATA
	HOXA3	Manually added from IPA-generated networks	cre-TATA
	HTR5A	Manually added from IPA-generated networks	cre-noTATA
	IFT172	Development of central nervous system (Table S1)	cre-noTATA
	MAP1B	Development of central nervous system (Table S1)	cre-noTATA
	PROC	Prothrombin activation pathway (Tables 1 and 2)	cre-TATA
	SERPINC1	Prothrombin activation pathway (Tables 1 and 2)	cre-noTATA
CRE half- sites present	APLP1	Development of central nervous system (Table S1)	h_-2998
	ATOH1	Development of central nervous system (Table S1)	ht_-4259 h_-2012 ht_-1575 h_-259 h_-521
	CD82	Development of central nervous system (Table S1)	ht_-3164 h_-37
	CELSR1	Development of central nervous system (Table S1)	ht_-1386
	ESR1	Manually added from IPA-generated networks	ht_-1183
	FAIM2	Development of central nervous system (Table S1)	h_-241 ht_-2523 h_-3959 ht_-420
	FGB	Prothrombin activation pathway (Tables 1 and 2)	ht_-4960
	FGG	Prothrombin activation pathway (Table 2)	ht_-4893
	F13A1	Prothrombin activation pathway (Table 1)	ht_-3814 ht_-440
	F2	Manually added node	
	F2R	Coagulation system (Table 2)	ht_-4399 h_-2699 ht_-1608
	GBX2	Development of central nervous system (Table S1)	h_-441 ht_-1634 HT_-4293
	OTP	Development of central nervous system (Table S1)	ht_-2976 HT_-3176
	PLXNA4	Development of central nervous system (Table S1)	ht_-1554 h_-244 H_-360
	RFX4	Development of central nervous system (Table S1)	h_-1610 ht_-418
	SLC1A2	Development of central nervous system (Table S1)	ht_-1349 ht_-2053 ht_-2370
	SMAD3	Manually added from IPA-generated networks	ht_-2932 h_-2467 ht_-1987 h_-997 h_-243
	SMO	Development of central nervous system (Table S1)	h_-352
	TAGLN3	Development of central nervous system (Table S1)	ht_-1762 ht_-1066 ht_-124 h_-908
	TFAP2C	Development of central nervous system (Table S1)	ht_-3518 ht_-3376 h_-3166 ht_-1866
	TRPV1	Development of central nervous system (Table S1)	h_-343 ht_-865 h_-1402
	TYRO3	Development of central nervous system (Table S1)	ht_-817 h_-39

CREB Target Prediction	Protein Symbol	Basis of Inclusion in Figure 3	CRE Description
Not found in database	NLGN4X	Development of central nervous system (Table S1)	

- All CREs predicted by *in silico* methods unless otherwise noted [23]
- H = conserved CRE half site (numbers depict location relative to transcription start site)
- h = CRE half site (numbers depict location relative to transcription start site)
- ht = CRE half site and presence of TATA box <300 bp downstream of CRE (numbers depict location relative to transcription start site)
- HT = Conserved CRE half site and presence of TATA box <300 bp downstream of CRE (numbers depict location relative to transcription start site)
- Other node in figures 4 and 5 not on this table: miR-132-3p

Table 4

Primer sequences used in qRT-PCR experiments.

Gene symbol	Forward primer (5' → 3')	Reverse primer (5' → 3')	Product size	RefSeq mRNA accession number
tnni1	AGGTTGGTGACTGGCGTAAG	GGGCCATTCTGAAGGTCAGT	127	XM_002667751.1
smad3	GAGCGCTGAACTTGAGACCGTGT	GCTCGTCCAGCTGTCCCGTC	341	NM_131571.2
serpine1	TGCCATGACAAAGCTAGGGG	GGCTCCATAGACAGTCTCGC	244	NM_182863.1
Tbp	GCCAACCGGTGGATCCTGCG	AAATGGGCAGGCCAGGCGTC	191	NM_200096.1

Table 5

Confirmation of gene expression changes by qRT-PCR.

Gene	Treatment	qRT-PCR (Fold change)			Microarray	
		Control mean \pm SEM	Treated mean \pm SEM	p-value	Fold change	p-value
<i>Tnni1</i>	15 μ M E2	1.0 \pm 0.2	0.3 \pm 0.1	0.017	0.328	0.035
<i>Snad3</i>	0.1 μ M BPA	1.0 \pm 0.0	0.9 \pm 0.0	0.030	0.847	0.027
<i>Serpinc1</i>	0.1 μ M BPA	1.0 \pm 0.0	1.1 \pm 0.0	0.002	1.133	0.001